Experimental Space Weathering: A coordinated LIBS, TEM, VIS and NIR/MIR study. A. N. Stojic[1], S. G. Pavlov[2], R. Wirth[3], A. Morlok[1], K. Markus[1], I. Weber[1], A. Schreiber[3], M. Sohn[4], H. Hiesinger[1], H.-W. Huebers[2], [1]Westfaelische Wilhelms Universitaet Muenster, Wilhelm – Klemm Str. 10, 48149 Muenster, Germany (a.stojic@uni-muenster.de), [2]German Aerospace Center (DLR), Institute of Optical Sensor Systems, Rutherfordstr. 2, 12489 Berlin, Germany, [3]Helmholtz-Zentrum Potsdam, Deutsches Geoforschungszentrum (GFZ), Telegrafenberg, 14473 Potsdam, Germany, [4]Hochschule Emden/Leer, Constantiaplatz 4, 26723 Emden, Germany

Introduction: Space weathering (SW) effects can be observed on all Solar System bodies, which lack a protective atmosphere [1, 2]. This includes asteroids, comets and satellites, but also planets, like Mercury, which has only a tenuous exosphere. An overview over all surface modifying influences is given by [3].

In our current study we follow the approach of [4,5] to simulate thermal effects of impacting (micro) meteorites on surface regolith material. We therefore irradiate pellets, comprised of comminuted olivine (ol) and pyroxene (px), with an infrared laser and investigate the altered areas. We use the focused ion beam (FIB) technique to cut out transmission electron (TEM) microscopy lamellae to investigate the consequences of irradiation damage at nanoscale. The remaining part of the pellet surface is investigated in the VIS, NIR, and MIR range. Our goal is to correlate the induced damage documented by means of TEM with the corresponding VIS/NIR and MIR spectra.

Experimental: Single crystals of olivine (Fo93) and pyroxene (En87) were ground in an agate mortar for 1hour. The resulting powder was not sieved and loosely pressed at 4 bar for 10 min. The pellet diameter is 10 mm and the surface was subsequently irradiated with a pulsed (~ 8 ns) laser operating at 1064 nm. The entire pellet surface was irradiated manually moving from spot to spot in 0.4 mm increments, each spot was irradiated 20 times at a fluence of ~ 2 Jcm^{-2}. Both mineral pellets were treated according to the procedure described above. The laser irradiation was carried out under a vacuum of 2×10^{-6} mbar. The pellets remained in the high vacuum chamber until one portion of a pellet was cut off to extract a TEM lamella and the remains of the pellet were investigated by infrared spectroscopy. Diffuse reflectance spectra were acquired in the VIS, NIR, and MIR range under vacuum, using a Bruker Vertex 70v and 80v. HAADF-STEM, SAED patterns, EDX measurements and BF micrographs were obtained using a FEI Tecnai G2 F20 X-Twin transmission electron microscope at the Geoforschungszentrum in Potsdam.

TEM Results: TEM observations show very distinct patterns for olivine and pyroxene, respectively (Figs. 1and 2).

Olivine. The developed weathering rim is locally twice as large as that developed on the pyroxene grain. Also different is the inherent structure of the rim. In olivine, the affected area is distributed evenly over the entire length of the TEM specimen. Nanoparticles are distributed in different layers and display diameters from 3 nm – 40 nm. The outermost layer on the weathered single crystal shows no TEM-resolvable metal nanoparticles. The structure of selected nanoparticles from other layers was identified by SAED and FFT of HRTEM images as body centered alpha Fe.

Pyroxene displays a range of different rims and shows only very few sites where nanoparticles could be identified. Also, nanoparticles are very small (<10 nm), rare and are distributed here and there throughout the weathered rim compared to olivine. A common feature in irradiated pyroxene grains are vesiculated rims with bubble sizes ranging from 50 – 200 nm.

VIS/NIR/MIR Results: Olivine contains only very little volatiles, e.g., traces of adsorbed water. Both, ol and px show darkening and reddening in their VIS/NIR spectra after irradiation. Our pyroxene specimen shows typical water absorption bands at 3 µm and a 2.7 µm absorption attributed to accessory clay minerals. The MIR range shows slight modifications in the Restrahlenbands (RB). Loss of intensity and peak broadening in the RB section of the MIR spectrum are the most prominent features probably attributed to increasing amorphization and/or also to topography change and the compaction of previously present pore space as a result of irradiation.

Discussion: Ol and px exhibit a different internal layering in their respective weathered rims when exposed to identical irradiation conditions. As inferred from previous spectral observations [e.g., 2,3,4,5], both, experimental laboratory study and asteroidal remote sensing, olivine is reddened more efficiently than px. This difference is also seen in TEM results from this study resulting in a distinct developed nanostratigraphy throughout the respective weathered rims. Although px contains only few metal nanoparticles, when compared to olivine, spectral reddening, though less pronounced than in ol, can also be observed in its VIS/NIR spectrum. This could be due to a sampling bias during FIB preparation (e.g., sampling a grain that has been exposed to irradiation less than its neighbors). Alternatively, it could probably also be explained by laboratory experiments conducted by [5] who suggest the major reddening agent in the VIS/NIR is the size fraction of particles <10 nm. The vesiculated rims occurring in pyroxene are linked to the volatile content in its crystal structure. Unfortunately, this makes a direct comparison to Mercurian regolith difficult as it is considered extremely dry compared to the volatile content of terrestrial samples. A generalization of the results obtained from the pyroxene sample is therefore difficult and requires further studies. A similar nanostratigraphy (as seen in the px TEM bright field (BF) micrographs), could probably occur in regolith grains that were slightly aqueously altered prior to being exposed to a heat source.

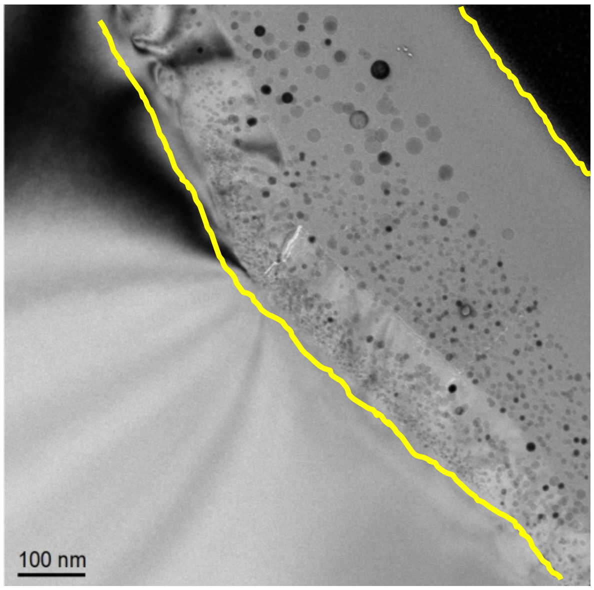

Figure 1: TEM bright field (BF) micrograph of ol FIB lamella after irradiation at ~ 2 Jcm^{-2}. FIB cut was carried out perpendicular into irradiated grain surface, thus a depth profile of the radiation damage is obtained. Weathered rim is framed in yellow underneath, the unscathed ol crystal (lower left) is preserved

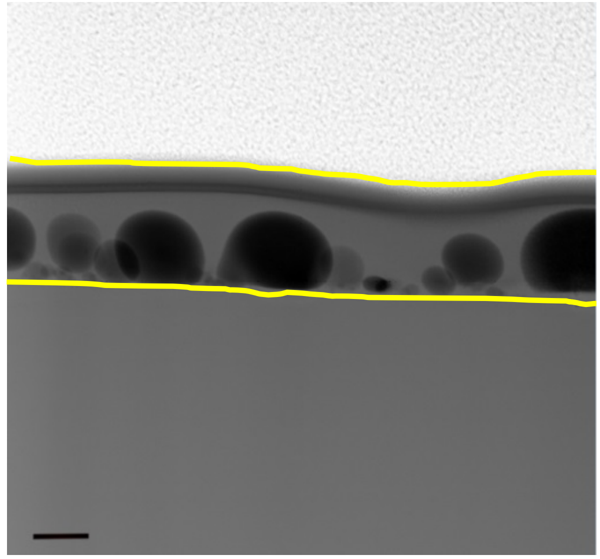

Figure 2: A high angle annular dark field (HAADF) Z - contrast TEM micrograph of a representative portion of the px weathered rim after irradiation. Here, a cross section of a radiation damage depth profile of the most abundant weathering feature in px is shown. Again the weathered rim (area affected by laser irradiation) is framed in yellow. Black holes are vesicles. Scale bar is 100 nm.

References:

[1] Pieters et al. (1993) *JGR: Planets*. 20817 - 20824 [2] Noble et al. (2001) *MAPS*. 31 - 42 [3] Domingue et al. (2014) *Space Sci Rev*, 121 – 214 [4] Yamada et al. (1999) *Earth, Planets Sp*. 1255 – 1265 [5] Sasaki et al. (2002) *Adv Sp Res*., 783 - 788 [6] Marchi et al. (2005) *Astron. Astrophys*., 769 – 775 [7] Noble et al. (2007) *Icarus*. 629 – 642

Additional Information: This work is funded by the DLR grant 50QW1302.